Comparison of Satellite-Deduced Cloud Heights with Indications from Radiosonde and Ground-Based Laser Measurements

W. L. SMITH[1]

Mesoscale Applications Branch, National Environmental Satellite Service, Madison, WI 53706

C. M. R. PLATT

Commonwealth Scientific and Industrial Research Organization, Division of Atmospheric Physics, Aspendale, Victoria, Australia

(Manuscript received 13 January 1978, in final form 2 September 1978)

ABSTRACT

Cloud altitudes specified from the Infrared Temperature Profile Radiometer on the Nimbus 5 satellite are compared with simultaneous observations by radiosonde and ground-based ranging measurements conducted with the lidar system at CSIRO in Aspendale, Victoria, Australia, during September 1976. The results show that the cloud altitudes deduced by the CO_2 channel absorption method are in general agreement with the lidar and radiosonde determinations, regardless of the cloud opacity and amount.

1. Introduction

Cloud heights and amounts (fractional coverage) were first determined from combined window and CO_2 absorption channel observations in 1969 as part of the process of determining vertical temperature soundings from low spatial resolution (200 km) Satellite Infrared Radiation Spectrometer (SIRS) measurements (Smith *et al.*, 1970). The advent of higher resolution spatially scanning radiometers (e.g., the 50 km VTPR instrument on the operational NOAA satellites, the 25 km ITPR on Nimbus 5 and the HIRS on the Nimbus 6) enabled soundings to be obtained without the explicit specification of cloud amount and height (Fritz *et al.*, 1972). However, because of the meteorological importance of cloud height and fractional coverage, the cloud parameters have been determined by the CO_2 channel absorption method along with the sounding information from the NimbusI TPR and HIRS experiments (Smith *et al.*, 1974b, 1975; Smith and Woolf, 1976). Unlike the method of specifying cloud altitudes from a temperature sounding and window channel brightness temperatures (assumed to be cloud-top temperatures), the specification of cloud height by CO_2 channel absorption does not require that the cloud be opaque and fill the satellite's field of view. The method may be applied to semitransparent cirrus cloud and small-element cumulus clouds as well as to dense stratiform cloud. This feature has been exploited by Chahine (1974) in conjunction with his iterative atmospheric parameter retrieval schemes and most recently by McCleese and Wilson (1976) in determining cloud properties from Nimbus Selective Chopper Radiometer (SCR) data.

Although the CO_2 channel absorption method has good scientific foundation, as yet there is little quantitative verification of the results of its application, mainly because there are no routine *in situ* observations of cloud pressure altitudes. As a result, while one of the authors (WLS) was on assignment to Australia during 1976, a limited sample was obtained of nearly coincident cloud height determinations from Nimbus 5 Infrared Temperature Profile Radiometer (ITPR) observations, the CSIRO lidar observations, and special radiosonde observations conducted at CSIRO in Aspendale, Victoria. This paper presents the comparison of cloud heights obtained from these three independent methods of observation.

2. Methods of observation

a. ITPR

The Infrared Temperature Profile Radiometer aboard the Nimbus 5 satellite has been described in detail by Smith *et al.* (1974a,b, 1975). Briefly, the instrument has seven different spectral channels and scans in grids to the right, center and left of the orbital track, each scan grid consisting of a 10×14 array (140) of contiguous elements (fields of view). The spatial resolution of each element and the distance between centers of the geographically contiguous elements is about 30 km.

[1] This research was done while on assignment to the CSIRO in Aspendale, Victoria.

0021-8952/78/1796-1802$5.00

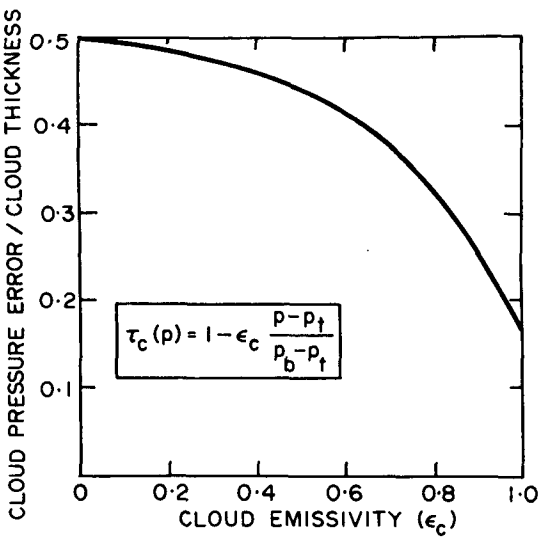

FIG. 1. Error due to infinitesimal cloud thickness assumption as a function of cloud opacity.

The procedure given by Smith *et al.* (1974b) for applying the CO_2 channel absorption method for cloud-height determination was adopted here. The cloud pressure is obtained by evaluating the expression

$$f(\nu_1,\nu_2,p_c)=\frac{R(\nu_1,N_1)-R(\nu_1,N_2)}{R(\nu_2,N_1)-R(\nu_2,N_2)} = \frac{\int_{p_c}^{p_0}\tau(\nu_1,p)\frac{dB[\nu_1,T(p)]}{dp}dp}{\int_{p_c}^{p_0}\tau(\nu_2,p)\frac{dB[\nu_2,T(p)]}{dp}dp}=f(\nu_1,\nu_2,p), \quad (1)$$

where $f(\nu_1,\nu_2,p)$ is the cloud pressure function to be evaluated; R is an earth outgoing radiance in a spectral channel whose central frequency is ν and whose field of view is characterized by cloud with fractional coverage N; and p_c is cloud pressure, p_0 surface pressure, τ the fractional transmittance of the atmosphere between space ($p=0$) and the atmospheric pressure level p, and B the Planck radiance for the temperature $T(p)$. As stated in (1), if the atmospheric temperature profile and the profiles of transmittance are known for two spectral channels whose outgoing radiance are sensitive to cloud, then the pressure of cloud within two fields of view can be specified from two radiance observations if only the cloud amount is different for the two fields of view. In practice, the pressure of cloud within a single field of view is obtained by utilizing an observed (or calculated) clear-column radiance for a nearby field of view and the temperature profile inferred from the clear-column radiances. In this case (1) becomes

$$f(\nu_1,\nu_2,p_c)=\frac{R(\nu_1)-R_c(\nu_1)}{R(\nu_2)-R_c(\nu_2)} = \frac{\int_{p_c}^{p_0}\tau(\nu_1,p)B'(\nu_1 p)dp}{\int_{p_c}^{p_0}\tau(\nu_2,p)B'(\nu_2 p)dp}=f(\nu_1,\nu_2,p), \quad (2)$$

where R_c is the clear-column radiance and $B'(\nu,p) = dB[\nu,T(p)]/dp$. The use of (2) instead of (1) helps suppress the effects of observational errors (the differences being ratioed are larger) and eliminates the requirement of having the same cloud height for the N_1 and N_2 observation conditions.

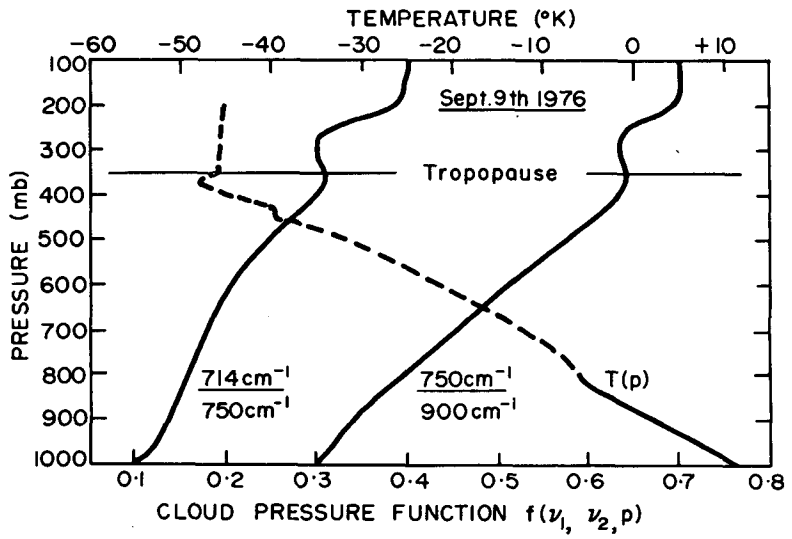

FIG. 2. Cloud pressure function for two ITPR channel combinations computed from the Aspendale temperature profile on 9 September 1976.

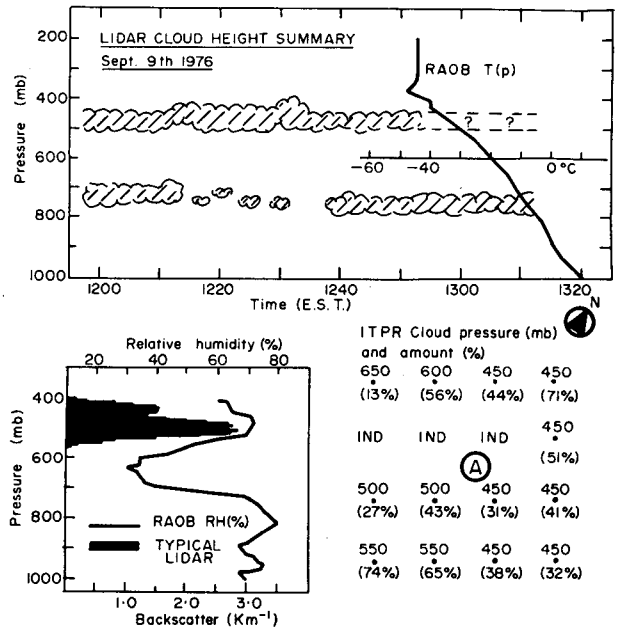

FIGURE 3.

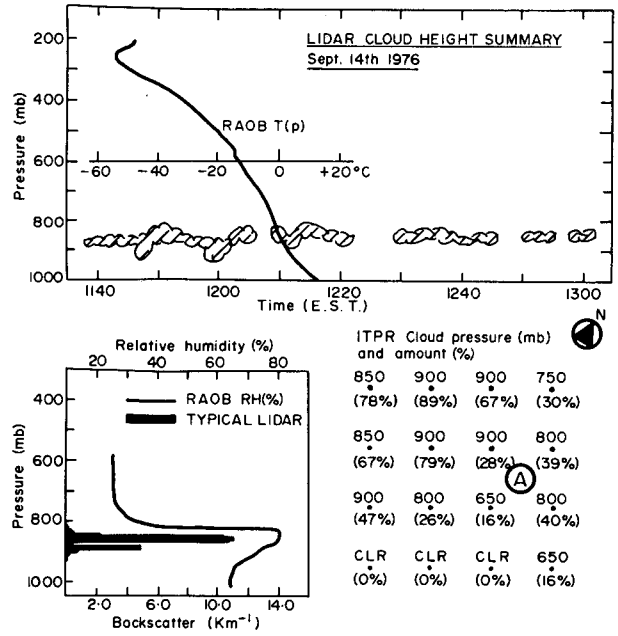

FIGURE 4.

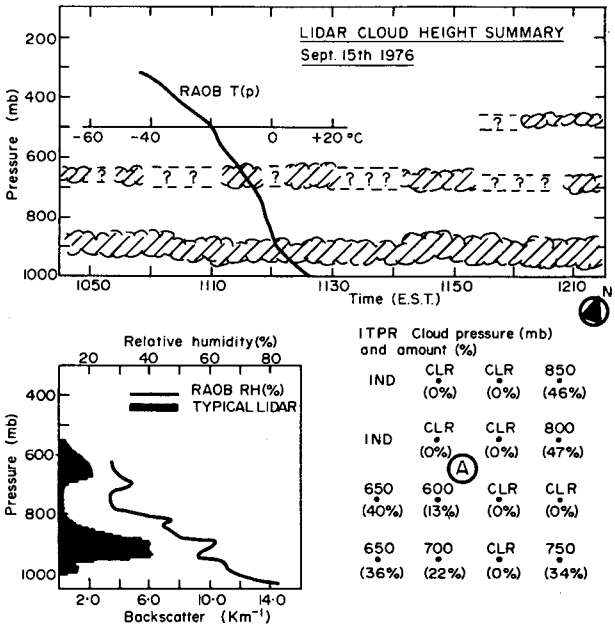

FIGURE 5.

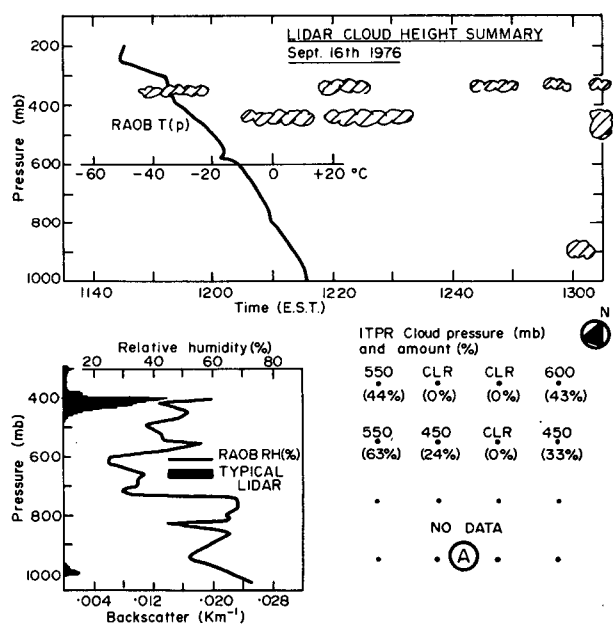

FIGURE 6.

FIGS. 3–11. Schematic summary of lidar cloud altitude observations and the Aspendale radiosonde temperature profile (top panel), typical lidar backscatter profile and radiosonde relative humidity profile (lower left panel), and satelliteborne ITPR cloud pressure and amount observations over the Aspendale vicinity (lower right panel).

As pointed out by Smith *et al.* (1974b), two basic assumptions are made in deriving Eq. (2): the cloud has infinitesimal thickness and the cloud transmissivity is the same for the two spectral channels employed. Fig. 1 is provided to illustrate the magnitude of error in cloud pressure due to the infinitesimal thickness assumption. The solid curve was the average result of calculations for a variety of cloud height, thickness and temperature profile conditions assuming the cloud transmittance has the functional form shown in this figure. There was little scatter around this mean result although a different cloud transmittance function would lead to a different shape of the curve. The significance of the result shown in Fig. 1 is that

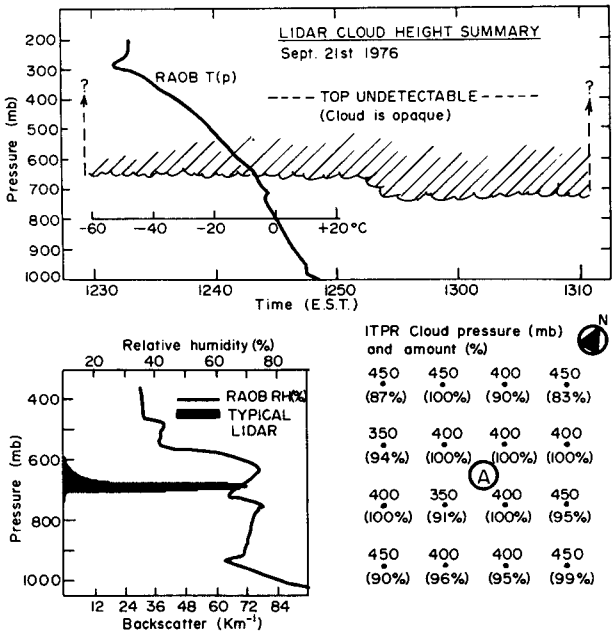

FIGURE 7.

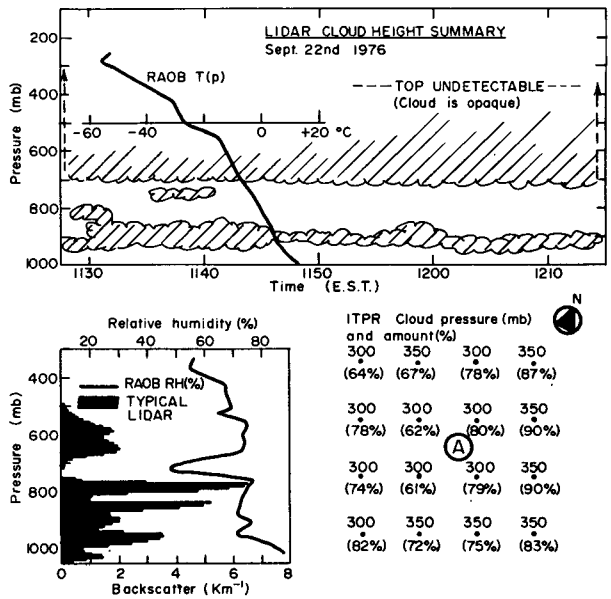

FIGURE 8.

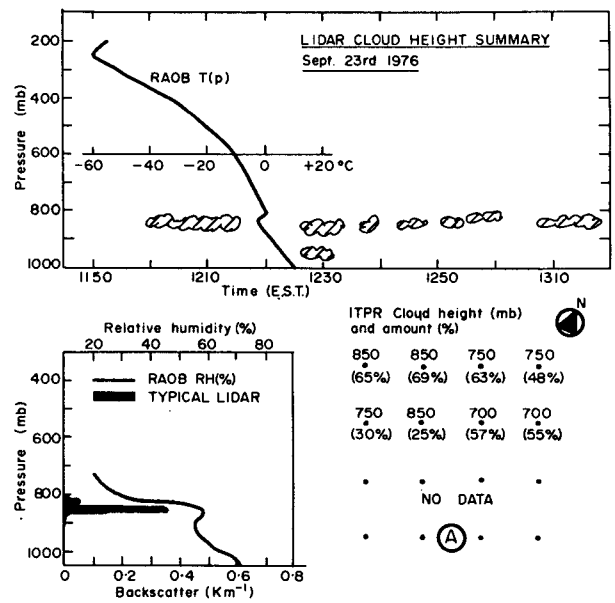

FIGURE 9.

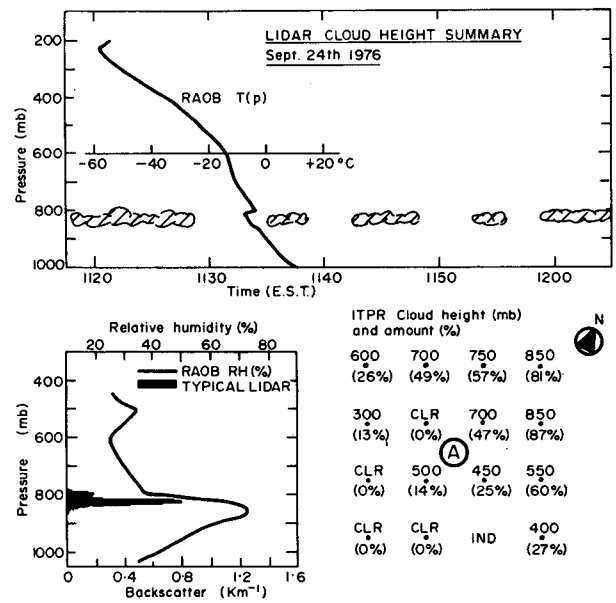

FIGURE 10.

FIGS. 3–11. *Continued*

the maximum error due to cloud thickness and opacity (emissivity) is half the cloud thickness and that is for an optically thin (small integrated emissivity) cloud. For an optically thick cloud, the error due to this assumption is smaller, as expected. The largest errors will be associated with geometrically thick but optically thin cirrus cloud.

To minimize errors due to violation of the second assumption, one uses spectrally close channels to minimize spectral differences in the real and imaginary parts of the index of refraction for ice crystals and water droplets. Calculations by Jacobowitz (1970) reveal that negligible errors due to spectral differences in cloud emissivity will occur when employing the ITPR 714 and 750 cm^{-1} channels for water and/or ice cloud determinations and the 750 and 900 cm^{-1} (window) channels for low-level dense water droplet cloud specifications.

Fig. 2 shows examples of cloud pressure functions calculated for two pairs of ITPR channels from the

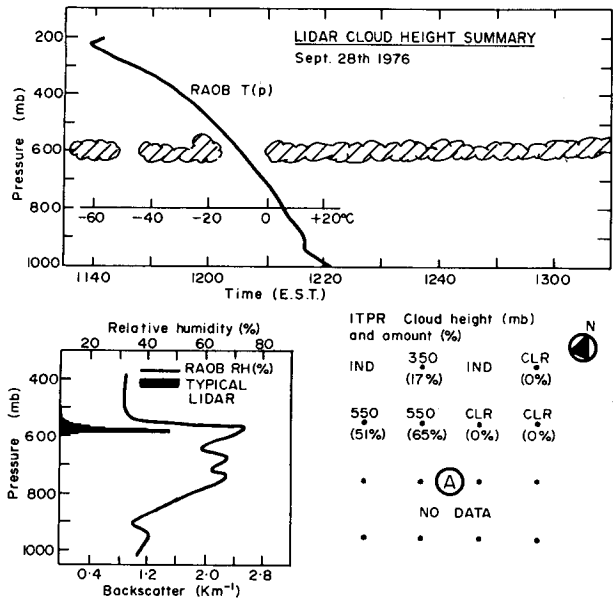

FIGURE 11.

FIGS. 3–11. *Continued*

Aspendale radiosonde observations of 9 September 1976. [The ITPR transmittance functions are given in Smith *et al.* (1974b).] As shown, the cloud pressure sensitivity (df/dp) is greater for the combination of the 11 μm window channel (900 cm^{-1}) and the most transparent 15 μm CO_2 band channel (750 cm^{-1}) than for the combination of two tropospheric sounding ITPR 15 μm CO_2 band channels, especially below the 500 mb level. However, since ice cloud is much more absorbent at 750 cm^{-1} than at 900 cm^{-1}, this pair of channels cannot be used to define the pressure altitude of cirrus clouds. Consequently, the 714/750 pair of radiance observations are used to define the pressure altitude of high clouds and the 750/900 pair is used to define the pressure altitude of middle and low clouds.

The procedure for calculating cloud pressure altitude may now be summarized as follows:

1) For a given cloud-obscured field of view for which the observed outgoing radiances are $R(\nu)$, obtain estimates of the clear-column radiances $R_c(\nu)$. The estimates can be obtained by one of three methods: (i) use a neighboring cloud-free observation, (ii) compute it using the "adjacent element N^*" technique (Smith *et al.*, 1968, 1972, 1976), or (iii) obtain it by a radiative transfer calculation, i.e.,

$$R_c(\nu)=B[\nu,T(p_0)]\tau(\nu,p_0)-\int_0^{p_0} B(\nu,T(p))[d\tau(\nu,p)/dp]dp,$$

using a radiosonde or satellite temperature profile. [In this study, method (i) was employed with corrections for angular differences between the cloudy field of view and the clear field of view due to limb-darkening being estimated by radiative transfer calculation using the Aspendale radiosonde observation.]

2) Calculate $f(\nu_1,\nu_2,p_c)$ from the observations $R(\nu)$ and $R_c(\nu)$, i.e., the lefthand side of Eq. (2).

3) Using a radiosonde (as was done in this study) or satellite observed temperature profile calculate the pressure function $f(\nu_1,\nu_2,p)$, i.e., the right-hand side of Eq. (2).

4) Using the 750/900 values, find that pressure (cloud pressure) for which $|f(\nu_1,\nu_2,p)-f(\nu_1,\nu_2,P_c)|$ is a minimum. If the resulting pressure is less than 500 mb use the 715/750 values to redefine the cloud pressure. If the discrepancy between the 750/900 and 715/750 values is greater than 300 mb, the solution is regarded as indeterminate due to multiple cloud levels within the field of view.

5) Compute an effective cloud amount (product of fractional coverage and cloud emissivity) using the relation (Smith *et al.*, 1974a)

$$N=\frac{R(w)-B[w,T(p_0)]}{B[w,T(p_c)]-B[w,T(p_0)]}, \tag{3}$$

where $R(w)$ is the observed cloud-obscured window channel (900 cm^{-1}) radiance and $T(p_0)$ and $T(p_c)$ are the surface and cloud temperatures, respectively.

Fig. 3 shows the first example of ITPR cloud heights determined by the technique described above. In this, and all cases to be shown, an ITPR cloud height (and amount) was calculated for every field of view within a 100 km radius of Aspendale, Victoria (the location of Aspendale relative to the ITPR data is shown by the circled A symbol on the data plot). As may be seen, for this case, the ITPR data indicated a cloud-top height of about 450–500 mb for Aspendale.

b. Laser

The heights of clouds over Aspendale were measured with the CSIRO lidar for a period of about an hour centered on the time of the Nimbus 5 satellite overpass time. The CSIRO lidar consists of a ruby laser (0.6943 μm) transmitter and a receiving telescope for observing the laser radiation backscattered from cloud particles. The range or height of the backscattered laser energy is given by the time delay between the transmitted and received energy [i.e., z(height) $=c$(speed of light) times Δt(time delay) divided by 2 (since energy travels to and from altitude z)]. Cloud bases and tops are detectable from the sharp increase and decrease of backscattered light with altitude, respectively. The abrupt change in backscatter is due to the much greater scattering efficiency of cloud water droplets and ice crystals than that of atmospheric molecules at the ruby laser wavelength.

The base and top heights of clouds were extracted from the laser backscattered signals for the entire observing period for each day of a Nimbus 5 overpass. In general, there was a lidar measurement every minute except near the time of the Nimbus 5 overpass when lidar observations were conducted about every 5 s.

Fig. 3 shows the cloud height summary for the entire lidar observing period for 9 September 1976, along with the temperature profile obtained by a special radiosonde released from Aspendale at the time at which the surface value is plotted. Question marks appear in the lidar determinations for upper clouds or upper portions of cloud where the signal is weak due to absorption by lower clouds or the lower portion of a thick cloud.

Along with the lidar cloud height summary a "typical" lidar return is given in each example where the return is expressed in terms of the backscatter (km^{-1}) as a function of altitude. Here the backscatter is merely the ratio of the received backscattered laser energy divided by the product of the emitted (or transmitted) laser energy and a calibration constant divided by the range (altitude) squared, i.e.,

$$B(\text{backscatter}) = b \exp\left[-2\int_0^z \alpha(z)dz\right] = L/(L_0K/R^2), \quad (4)$$

where b is the volume backscatter coefficient (km^{-1}), α the volume extinction coefficient (km^{-1}), L_0 the emitted laser energy, L the received laser energy, K an instrument constant and R^2 the square of the range or altitude of measurement. Fig. 3 shows the observed laser backscatter for a shot (denoted as TYPICAL LIDAR) conducted when there was no lower cloud. As can be seen for this individual shot, the only significant backscatter is in the 400–550 mb layer.

c. *Radiosonde*

Finally, radiosonde measurements were made to measure the heights of cloud over Aspendale. In this case, the relative humidity obtained from the radiosonde temperature and dew point observations are used to diagnose the existence of cloud since the humidity is high within cloud layers. Again, Fig. 3 serves as an example where the radiosonde (RAOB) relative humidity (RH) is high (>60%) below 700 mb, indicating low cloud, and also high in the 500–400 mb layer, indicating a high cirrus layer over the lower cloud deck.

3. Results

Figs. 3–11 show the comparison of cloud-height signatures obtained by the satellite, lidar and radiosonde observing methods. Noteworthy is the overall agreement in the vertical cloud structure indicated by the radiosonde relative humidity and the lidar backscatter observations. The two exceptions to this agreement are shown in Figs. 5 and 7 which are cases of dense, thick stratus cloud. In these cases the lidar energy getting into the cloud is absorbed by the cloud so that only a signature of the cloud base is achieved.

TABLE 1. Summary of ITPR, radiosonde and lidar indicated cloud-top pressure altitudes for Aspendale, Victoria (Australia).

Date September	Radiosonde Pressure (mb)	Lidar Pressure (mb)	ITPR* Two-channel method Pressure	ITPR* Two-channel method Amount (%)
9	420(?)	440	450	31
14	830	830	800	39
15	700(?)	630	600	13
16	400	420(?)	450	24
21	460(?)	—	400	100
22	330	—	300	80
23	850	830	850	25
24	500	800(?)	500	14
28	550	550	550	65

* Values chosen are those which are in best agreement with lidar observations.

Table 1 summarizes the comparison of radiosonde, lidar and Satellite Infrared Absorption (ITPR) observations of cloud-top pressure altitude. As can be seen, there is good agreement between the radiosonde, lidar and CO_2 absorption channel observations.

Acknowledgments. The authors wish to thank Mr. M. Dilley and Dr. Ian Barton of CSIRO for their help in conducting the ground-based measurements and Messrs. L. Mannello and H. Woolf of NESS for acquiring the satellite data.

REFERENCES

Chahine, M. T., 1974: Remote sounding of cloudy atmospheres. I. The single cloud layer. *J. Atmos. Sci.*, **31**, 233–243.

Fritz, S., D. Q. Wark, H. E. Fleming, W. L. Smith, H. J. Jacobowitz, D. T. Hilleary and J. C. Alishouse, 1972: Temperature sounding from satellites. NOAA Tech. Rep. NESS 59, 49 pp.

Jacobowitz, H. J., 1970: Emission scattering and absorption of radiation in cirrus cloud layers. Ph.D. thesis, Massachusetts Institute of Technology, 181 pp.

McCleese, D. J., and H. M. Wilson, 1976: Cloud top heights from temperature sounding instruments. *Quart. J. Roy. Meteor. Soc.*, **102**, 781–790.

Smith, W. L., 1968: An improved method for calculating tropospheric temperature and moisture from satellite radiometer measurements. *Mon. Wea. Rev.*, **96**, 387–396.

——, and H. M. Woolf, 1976: The use of eigenvectors of statistical covariance matrices for interpreting satellite sounding radiometer observations. *J. Atmos. Sci.*, **33**, 1127–1140.

——, —— and W. J. Jacob, 1970: A regression method for obtaining real-time temperature and geopotential height profiles from satellite spectrometer measurements and its

application to Nimbus 3 SIRS observations. *Mon. Wea. Rev.*, **98**, 604–611.

——, ——, C. M. Hayden and W. C. Shen, 1975: Nimbus 5 sounder data processing system part II: Results. NOAA Tech. Memo. NESS 71, 102 pp.

——, D. T. Hilleary, J. C. Fischer, H. B. Howell and H. M. Woolf, 1974a: The Nimbus-5 ITPR Experiment. *Appl. Opt.*, **13**, 499–506.

——, H. M. Woolf, P. G. Abel, C. M. Hayden, M. Chalfant and N. Grody, 1974b: Nimbus 5 sounder data processing system Part I: Measurement characteristics and data reduction procedures. NOAA Tech. Memo. NESS 57, 99 pp.

——, D. T. Hilleary, E. C. Baldwin, W. J. Jacob, H. Jacobowitz, G. Nelson, S. D. Soules and D. Q. Wark, 1972: The airborne ITPR brassboard experiment. NOAA Tech. Rep., NESS 58, 74 pp.